UltraPower: Powering Tangible & Wearable Devices with Focused Ultrasound

Rafael Morales
Ultraleap Ltd
Bristol, United Kingdom
rafael.morales@ultraleap.com

Asier Marzo
Universidad Pública de Navarra
Pamplona, Spain
asier.marzo@unavarra.es

Euan Freeman
University of Glasgow
Glasgow, United Kingdom
euan.freeman@glasgow.ac.uk

William Frier
Ultraleap Ltd
Bristol, United Kingdom
william.frier@ultraleap.com

Orestis Georgiou
Ultraleap Ltd
Bristol, United Kingdom
orestis.georgiou@ultraleap.com

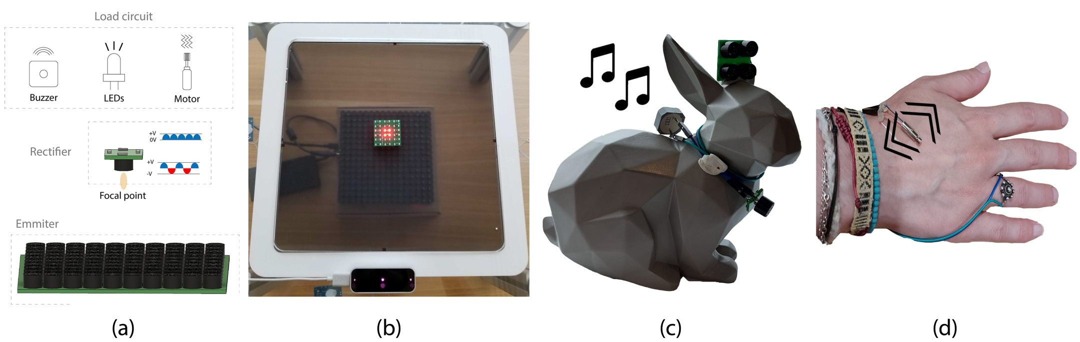

Figure 1: UltraPower uses focused ultrasound to wirelessly transfer power to components in tangible and wearable devices (a): e.g., lights in a tabletop tangible object (b), loudspeakers on a physical object (c), and vibration motors in wearable devices (d).

ABSTRACT

Wireless power transfer creates new opportunities for interaction with tangible and wearable devices, by freeing designers from the constraints of an integrated power source. We explore the use of focused ultrasound as a means of transferring power to a distal device, transforming passive props into dynamic active objects. We analyse the ability to transfer power from an ultrasound array commonly used for mid-air haptic feedback and investigate the practical challenges of ultrasonic power transfer (e.g., receiving and rectifying energy from sound waves). We also explore the ability to power electronic components and multimodal actuators such as lights, speakers and motors. Finally, we describe exemplar wearable and tangible device prototypes that are activated by *UltraPower*, illustrating the potential applications of this novel technology.

CCS CONCEPTS

• **Human-centered computing** → **Interaction devices**; • **Hardware** → *Power and energy*; *Wireless devices.*

KEYWORDS

Energy; Ultrasound; Tangible Device; Wearable Device; Wireless Power Transfer

ACM Reference Format:

Rafael Morales, Asier Marzo, Euan Freeman, William Frier, and Orestis Georgiou. 2021. UltraPower: Powering Tangible & Wearable Devices with Focused Ultrasound. In *Fifthteenth International Conference on Tangible, Embedded, and Embodied Interaction (TEI '21), February 14–17, 2021, Salzburg, Austria.* ACM, New York, NY, USA, 13 pages. https://doi.org/10.1145/3430524.3440620

1 INTRODUCTION

Power is a crucial requirement for almost every interactive computing device. Provision of power has a significant impact on the device form factor and use: batteries need to be integrated, charged or replaced, whereas wired alternatives may constrain the range of interactions with the device. Moreover, power integration continues to affect a device after its functional life-cycle has ended as it can prevent or increase the cost of its recycling. To that end, wireless power transfer (WPT) is an appealing alternative, pioneered by N. Tesla in the 1890s, whereby power is transferred without physical

TEI '21, February 14–17, 2021, Salzburg, Austria

ACM ISBN 978-1-4503-8213-7/21/02…$15.00
https://doi.org/10.1145/3430524.3440620

contact to a device, allowing for its untethered operation without an integrated power source.

Power can be wirelessly transmitted and received by a device in a variety of ways. Currently, resonant inductive coupling is a ubiquitous example of WPT, and is widely used by many modern mobile devices for charging purposes. Other WPT methods include capacitative coupling, magnetodynamic coupling, lasers, and focusing of radio, sound or ultrasound waves [62, 73, 78, 83]. Since many WPT-enabled devices require no battery replacement, they can be cheaper and easier to manufacture, operate, and recycle, and can be better weatherproofed due to the lack of a battery access panel or power connector. To that end, WPT has enabled a plethora of interesting new interactive use cases and applications within the space of human-computer interaction (HCI) and the Internet of Things (IoT) [10, 17, 34, 50, 65, 78, 80].

In this paper, we advance WPT-enabled HCI applications through the use of focused ultrasound. Focused ultrasound using electronically controlled phased arrays has received a lot of interest in HCI for mid-air haptic feedback [8, 22, 33, 51, 70] and acoustically levitated display elements [20, 21, 46, 52, 58, 61]. These novel interfaces typically use a collection of piezoelectric transducers (speakers) to emit and focus ultrasound waves (typically at 40 kHz), resulting in focal points with high sound pressure level, and thus a high energy density. The same piezoelectric elements can also be used as receivers that transduce the incoming ultrasound waves into electrical energy. This technology is not new and has primarily been used in engineering and medical applications such as powering medical implants and IoT sensors. Airborne ultrasound WPT has a small form factor (a few centimetres) [32], can achieve power conversion efficiencies of the order of 35% [82], and can be encoded with additional information enabling control and data transfer applications beyond simple switching on/off sensors and actuators [66]. Consequently, we argue that ultrasound WPT is a strong candidate for HCI applications. Thereby, a transmitting ultrasonic phased array can generate localised focal points of high acoustic pressure that can then be harvested by distal ultrasonic receivers that use the collected energy for storage or consumption. The receivers do not need to be powered themselves to do this and can passively transduce electrical current from the localised sound pressure, transforming passive props into dynamic active objects. Here, we will explore the potential of this basic principle and investigate how focused ultrasound can be used for WPT in a range of interactive devices such as tangibles and wearables— a concept that we call *UltraPower*.

We propose and demonstrate that *UltraPower* can be used to power small interactive devices and electronic components in a robust and precisely targeted wireless manner. This is achieved by first leveraging the precision and update speeds of transmitting ultrasonic phased arrays in modulating ultrasound in both space and time, thus enabling spatial, time and frequency multiplexing. Other WPT technologies do not afford such high levels of precision and variety; an important and exploitable capability in multiple HCI applications. For example, while electromagnetic (EM) radiation energy from radio and infrared waves can be easily harvested, beam-steering and accurate focusing of EM energy cannot be easily achieved to target specific devices due to the large wavelengths. Recent 5G EM spectrum in the 60 GHz with multiple antenna elements is expected to be able to achieve sub-centimetre focusing and simultaneously target two nearby devices by the transmitter; however, this has not yet been demonstrated for WPT applications. *UltraPower* can create multiple targeted focal points with mm precision. Second, through experimentation and rapid prototyping we demonstrate and discuss issues related to the reception and rectification of ultrasonic energy. Knowing the capabilities, design space, and limitations of *UltraPower* is paramount for HCI and UX designers. We therefore characterise how *UltraPower* performance varies with distance, load, input power, and focusing accuracy; thus affecting interaction use cases in tangible and wearable applications that do not need an on-board power source anymore. Despite our testing and prototyping efforts presented in this paper, it is clear that we have only just scratched the surface of this emerging field and hope that our work motivates further experimentation as well as user-centred application development using *UltraPower*.

2 RELATED WORK

UltraPower uses focused ultrasound from an array of transducers to precisely deliver power to another device, allowing the creation of novel tangible user interfaces and wearable devices. We give an overview of ultrasound arrays and their primary interactive applications, common techniques for wireless power transfer, and their limited use in tangible and wearable interaction techniques.

2.1 Ultrasonic Phased Arrays

UltraPower is based on the principle of using airborne ultrasound generated by an array of emitters to transfer energy to a distal receiver. A typical 40 kHz piezoelectric transducer (a wavelength of $\lambda = 8.6$ mm) produces 20 Pa of sound pressure at a distance of 30 cm [33]. A receiving element would then be excited by the resulting pressure amplitude oscillation, thus producing a power output signal. A single ultrasonic emitter generates low-amplitude pressure with a fixed spatial pattern. However, arrays of dozens or hundreds of emitters with individual phase control can generate orders of magnitude more localised pressure due to constructive and destructive wave interference. Phased-array focusing techniques can be used to modulate the phase and amplitude of each individual transducer so that each emitted spherical wave arrives at the target positions in-phase and thus will add constructively to increase the total pressure.

Applications of focused ultrasound have received significant interest in HCI research during the last few years, most notably mid-air haptic feedback. Mid-air haptic feedback using a phased ultrasound array was first demonstrated by Iwamoto *et al.* [33] and later by Carter *et al.* [8]. The acoustic energy in a focal point exerts pressure against the skin and, when modulated appropriately, the localised pressure variations stimulate touch receptors in the skin. Several modulation methods have been explored for transferring this acoustic energy to touch receptors (e.g., amplitude [8], lateral [70] and spatiotemporal modulation [22]). Modulated focal points thus become the building blocks of complex haptic sensations, enabling users to feel 3D shapes [42] and interactive mid-air widgets (e.g., [19, 27, 41]). Two other emerging applications of airborne ultrasonic phased-arrays are displays made of acoustically levitated particles [23, 28, 44, 58] and targeted parametric audio delivery [6, 59]. Modulation techniques from mid-air haptics, parametric audio and levitation can be transfered to the WPT domain. Our aim with *UltraPower* is to explore new interactive applications of airborne ultrasound to wirelessly power interactive devices by leveraging existing hardware, software and operating principles.

Emerging application areas have prompted new research into the safety of in-air ultrasound. Ultrasound is a non-ionising radiation and is therefore not associated with any form of cell mutation, cancer-causing effects, or heating effects. Skin is a very poor absorber of in-air ultrasound and reflects 99.9% of the energy at 40 kHz [33]. As such, the effects of ultrasound to human hearing would be our main concern. A recent review of ultrasound standards [38] provides a deeper discussion on this topic. Our 16x16 array is able to generate a maximum of 163.5 dB of peak sound pressure level (SPL) (3000 Pa) , or equivalently a sound intensity of 22.5 kW/m^2 at a focal point located 20 cm above the array which is in the order of λ^3. This represents a significant amount of energy density. However, outside of the focal point, the sound pressure drops very rapidly and is estimated to be approximately 110 dB (6 Pa) at a distance of 60 cm from the focal point. Further absorption and reflections on the environment can reduce this SPL further. Recent studies have not found safety concerns or negative effect on hearing sensitivity thresholds [7, 14].

2.2 Wireless Power Transfer

Wireless power transfer (WPT) is the principle of transferring power between two devices without physical contact. WPT capabilities are already present in many commercial products (e.g., for wireless charging and contactless payments) [2, 24] and novel approaches are expanding the range and capabilities of power transfer, leading to applications like batteryless Internet of Things devices [17]. Over short distances, power can be transferred using electromagnetic radiation; e.g., inductive coupling between wire coils or capacitive coupling between metal electrodes. Such approaches are ubiquitously used for charging mobile devices. Over larger distances (e.g., several metres), energy can be transferred using a variety of radiation types: including microwaves [48], laser beams [34, 71] or radio waves [17]. Ambient energy harvesting is a closely related concept, where devices gather energy from existing background radiation in the environment (e.g., vibration, temperature gradients, wind, sunlight, and even WiFi) [13, 25]. The defining characteristics of WPT, which we use in this work, are the use of a dedicated power emitter and receiver at which energy is targeted.

Ultrasonic WPT (uWPT) is an emerging form of WPT that has operational advantages in the mid-field range, filling a gap between near-field electromagnetic WPT and far-field beamforming approaches. uWPT has mostly been used to deliver power and data to implantable devices inside the human body [1, 69] like pacemakers, which require just a few microwatts of power to function [67]. Ishiyama *et al.* [32] were the first to show the feasibility of uWPT through air, rather than biological tissue. As research interest into uWPT grew, efficiency became the main concern. Improvements in ultrasound transducer design and signal processing have since led to significant improvements in energy transfer efficiency and targeting precision, e.g., as demonstrated by Tseng *et al.* [74]. Rekhi *et al.* [66] investigated the feasibility of uWPT for Internet of Things applications, showing the ability to transfer microwatts of energy over a distance of 1 m. This represents a much higher power density compared to state-of-the-art equivalent radio frequency WPT over a comparable range [9]. Furthermore, prototypes and simulations presented by Tseng *et al.* [73] and Nagaya *et al.* [56] have shown that uWPT efficiency can be drastically improved by using multiple receiving elements instead of one. For example, Zaid *et al.* [82] have achieved a power conversion efficiency of 34% and anticipate further improvements based on thermal insulation.

Several works have considered the use of WPT to enable novel interactions with computing devices. For example, researchers have investigated WPT for interaction with wearables and smartphones using inductive coupling [80], activity detection with radio tags [83], actuated papercraft using inductive coupling [84], tangible objects powered by radio waves [49] and near-field communication (NFC) [77], and inductive coupling between items of clothing [50]. In this paper, we investigate the use of uWPT to power tangible and wearable devices with a scope of increasing the range of interactive applications as contrasted to the near-field WPT approaches previously explored.

2.3 Interactive Tangible and Wearable Devices

Tangible user interface objects can be *active*, utilising electrical components to actuate themselves for movement across a surface [15, 49, 57, 60, 63] and for interaction feedback across many output modalities [5, 37, 76]. These are a compelling alternative to traditional *passive* tangibles, which are typically only augmented by adjacent screens or projection surfaces (e.g., [35, 53, 54]). Active tangibles require power which increases their complexity and may constrain object form factor. A limited body of research has investigated powerless alternatives for creating active tangible devices. For example, *Madgets* [79] manipulated magnetic fields to actuate magnets embedded in tangible controls so that discrete components (e.g., a slider handle) or the entire object could be moved. *Geckos* [39] and *FluxPaper* [60] made similar use of magnets to add input sensing and output actuation capabilities to otherwise powerless objects.

Most relevant to our work is the *Things that Hover* [49] system, a tabletop interface that used electromagnetic WPT to create self-hovering tangible objects. Electromagnetic energy was rectified and used to power an integrated piezoelectric blower, which raised the object off the table surface to provide simple actuation capabilities. *Project Zanzibar* [77] used NFC to track the position and orientation of tangible objects atop a tabletop mat. A suitable rectifier can harvest energy from the NFC mat, delivering power to electrical components. In this work, we investigate ultrasound WPT as a compelling alternative to near-field WPT. Focused ultrasound can transfer usable energy over a much greater distance, supporting off-surface interaction [11] in mid-air too. Furthermore, ultrasound can be very precisely targeted, enabling the selective activation of individual components in one device, or activating one of many devices.

Wearable devices are interactive devices worn on the body, expanding input and output options for computer interfaces. Wrist-worn form factors and glasses are the most common consumer wearables, although others have also demonstrated interactive rings [4, 19, 26, 72], fingernail attachments [36, 47],and even tiny robots that crawl across clothing [12]. A limiting element for novel wearable form factors is their need for an integrated power source and having to remove them for charging. *UltraPower* could be used to deliver power to wearable devices, even through clothing [20], which would enable the design of novel wearable devices without the form factor constraints of an integrated power source.

3 ULTRAPOWER

UltraPower is a wireless power transfer system that uses focused ultrasound from a phased array to precisely deliver power to targeted electronic components for visual, auditory and tactile output. Ultrasound as a transfer mechanism allows power to be delivered across a large interactive area, making *UltraPower* suitable for a variety of tangible, wearable and desktop interaction scenarios. Through its use of simple and readily available components, *UltraPower* allows designers and makers to add interactive capabilities to inanimate objects, without the need for an integrated or connected power source. Removing the power source alleviates design constraints, allowing interactive electronics to be added to existing physical objects, novel or flexible form factors, and textiles.

An *UltraPower* system consists of three main components (see Figure 2): (1) a phased array of ultrasonic transducers, which generates a sound pressure field with focal points at the desired target positions; (2) a receiver and a rectifier circuit, which converts AC voltage into DC voltage; and (3) a load circuit with output components that consume the received power (e.g., LEDs, motors, actuators and buzzers). Additional components such as energy storage and management modules can also be included but will not be considered here. We now describe each of these parts in more detail, using our own implementation as a case study for fabricating *UltraPower* prototypes.

3.1 Ultrasound Phased Array

Our implementation uses a 40 kHz ultrasound array (Ultraleap UHEV1) with 16x16 transducers. This can create focal points with similar diameter to the in-air wavelength λ. These points are smaller than the transducer diameter (10 mm), allowing us to precisely direct energy to individual receiving transducers, so that they can be activated independently, without accidentally activating adjacent receivers. In the simplest use case, an ultrasound focal point can be used to turn on an output component (by transferring power to it). However, focal points can also be modulated with bandwidths in the kHz range, allowing transfer of data and signals for more complex control.

A desirable characteristic of an ultrasound array is the ability to produce multiple focal points simultaneously so that multiple devices can be powered at the same time (e.g., tangibles held in both hands). This can be achieved using multiple focal point methods [42], thus allowing multiple components to be simultaneously activated. The total acoustic pressure that a phased array can produce is approximately constant, meaning that the maximum amplitude at two points will be half of the achievable amplitude of a single-point, and so on [52].

3.2 Receivers and Rectifier Circuits

3.2.1 Receiving Transducers. A receiving transducer will be excited by a focal point where the acoustic energy is present as a pressure oscillation, converting that energy into AC electricity. The amount of electrical output will be proportional to the focal point pressure and the receiver's sensitivity S. Sensitivity is therefore an important parameter for operational efficiency, affecting the overall performance of an *UltraPower* system. To that end, we have tested the sensitivity of three common low-cost receiver transducers using the pulse-echo method. Output pulses were sent from a Murata MA40S4T transducer (as used by the UHEV1 array). Each receiving transducer was placed 10 cm away and the voltage change at the receiving end was measured using an oscilloscope. Our measurement results are shown in Table 1. The MSO-P1040H07R transducer was the most sensitive by a margin of over 10 dB. This is therefore our recommended option for an *UltraPower* receiver.

Receiver Transducer	Diameter	Sensitivity
Murata MA40S4R	10 mm	-65.4 dB±1
Manorshi MSO-P1040H07R	10 mm	-53.6 dB±2
Manorshi MSO-P1640H12R	16 mm	-71.5 dB±2

Table 1: Sensitivity of low-cost receiving transducers.

The orientation of a receiving transducer in relation to the ultrasound source also has an impact on received power since this affects how much pressure enters the rectifier. For typical piston-shaped receivers of 10 mm diameter (as used in this work) at 15°, the received power is typically reduced by 10%; 20% at 22°, 50% at 41°and 90% at 67°. Product data-sheets and published measurements can provide more detailed information about directivity [3]

Directivity thus has implications for receiver placement on an interactive device and for the design of HCI applications. Namely, the receiver transducers should be approximately facing towards the ultrasound source; however, there is sufficient flexibility to support dynamic and mobile interactions. For example, a device worn on the wrist will require receivers facing the emitter array, which will typically be downwards in a desktop interaction context. Multiple receivers can also be used to widen the range in which high levels of power can be received. Similarly, receivers placed at different angles can be used to power specific components, depending on the orientation of the device.

For *UltraPower* to be integrated seamlessly into a device, it may be desirable that receivers are not exposed on the device exterior. Fortunately, ultrasound can penetrate various materials with little pressure loss [8, 52]. Freeman *et al.* [20] investigated the effects of acoustically transparent materials on the focal point amplitude. For example, at a distance of 15 cm, a 40 kHz signal attenuates its amplitude pressure by 22% when passing through acrylic felt, 15% for polyester, 10% for rayon and 2% for organza. This makes *UltraPower* suitable for powering devices that are in pockets or worn beneath clothing. Perforated sheets or mesh-like materials also allow ultrasound to pass through with low attenuation. For example, 5–20% of pressure is lost when passing 40 kHz ultrasound through a steel mesh, allowing *UltraPower* receivers to be placed inside robust and rigid enclosures [45].

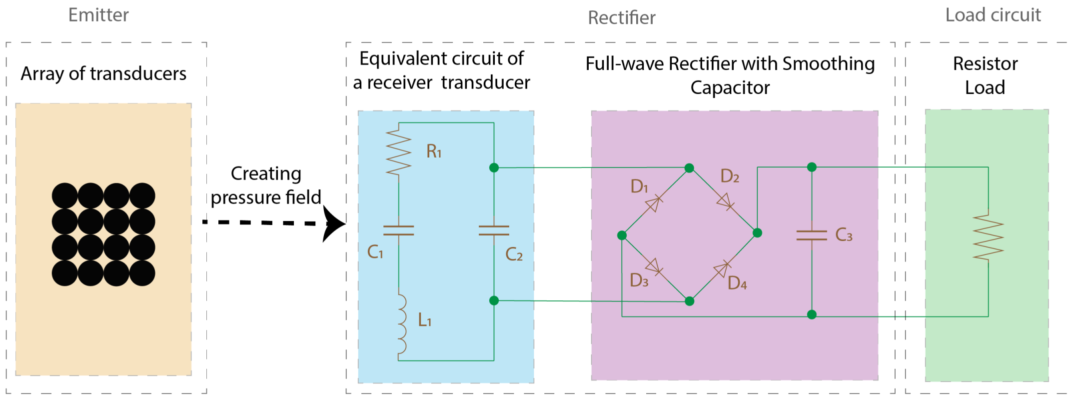

Figure 2: Overview of an *UltraPower* system. An ultrasonic phased-array generates focal points at target positions. Focal points consist of rapidly oscillating pressure, which a receiving transducer will transduce into an alternating current (AC). This gets rectified and smoothed to obtain a direct current (DC), capable of powering a load circuit (e.g., LEDs, buzzers or motors).

3.2.2 Rectifier Circuits. While a receiver will transduce acoustic energy into an alternating current (AC), a rectifier circuit is necessary to turn this into direct current (DC). A simple rectifier circuit can be created using four Schottky diodes, a capacitor and a receiver transducer (as shown in Figure 2). Instructions on how to build your own rectifier are readily available on many online websites. We recommend choosing Schottky diodes with a low forward voltage (<300 mV) to maximise the amount of power available to the output components.

Focal points are approximately $\lambda = 8.6$ mm diameter for 40 kHz ultrasound, so the receiver transducers need to be targeted by the transmitting phased array with an accuracy of $\lambda/2$ in order to transfer power effectively. This is especially important for tangible and wearable devices that will move and be reoriented during interaction. Fortunately, state-of-the-art ultrasound arrays can reposition focal points rapidly and with sub-millimetre precision; for example, the UHEV1 array used in this work can update a focal point position up to 16,000 times per second. Evaluation of the tracking and targeting accuracy required for efficient WPT is beyond the scope of this paper, however, we address this in the final discussion.

3.3 Interactive Components

UltraPower devices can use the rectified power to drive a variety of electrical components, supporting a range of interactive experiences with visual, auditory and tactile output, and input via buttons and other sensors. Briefly described below are three types of output component explored in our technical evaluation and application demonstrators: LEDs, buzzers, and micro-motors (Figure 3). These represent low-, medium- and high-power components, respectively. By characterising their performance in this work, we can estimate their operational range and capabilities for being integrated in an *UltraPower* system. Moreover, other components can be benchmarked against them, to assess their suitability and performance for ultrasonic WPT. Before discussing their evaluation and use in our prototypes and demos, we first describe how they can be integrated and used in an *UltraPower* device.

3.3.1 Buzzers. A piezo buzzer is essentially a small speaker, operating with a very low input power with the drawback of a narrower frequency range. Buzzers can be active or passive. Active buzzers contain an oscillating circuit and thus only require a DC current to produce sound; however, they play just a single frequency tone and only their amplitude can be controlled. In an *UltraPower* system, an active buzzer's output amplitude can be controlled by adjusting the amplitude of the focal point targeting its receiver.

Passive buzzers require an oscillating current, which will be directly transduced into audible sound. *UltraPower* systems can modulate the focal point amplitude, resulting in pressure oscillations that will be reproduced by the buzzer. This would enable a range of tones to be played from the receiving device. Whilst implementing our *UltraPower* prototypes, we tested two active buzzers and a passive piezoelectic buzzer (Figure 3a): a Sonitron *SMA-13* active buzzer, a Sonitron *SMA-17* active buzzer, and an unbranded passive piezoelectric buzzer. Their minimum operating power requirements ranged from 3–5 mW. All successfully produced audible output when their receiving transducer was activated by a focal point.

3.3.2 Motors. Motors can use received power to actuate other components or materials. The most appropriate motors will be those that require low voltage and current. The Precision Microdrives *Pico Vibe* motor was evaluated as a suitable motor that can be activated by *UltraPower*. Its key specifications from the datasheet are an operating voltage of 1.5V, current of 17mA (i.e., 25.5mW), resulting in driving speeds of up to 10700 rpm. In testing, we used the rotation of this motor to deliver haptic feedback in the form of tactile vibrations by attaching an eccentric mass to its axis. Using gears, these motors could also be used to add locomotion to small devices, or to elicit change from a shape-changing tangible.

3.3.3 Lights. A wide range of LEDs can be activated by *UltraPower* at meter distances. For instance, regular high-brightness, surface-mount or through-hole LEDs can be activated. We employed LEDs with low forward voltage (V_f) to improve control of the brightness and maximize the light output. Note that LEDs can be directly connected to a receiver transducer given that they act as a diode

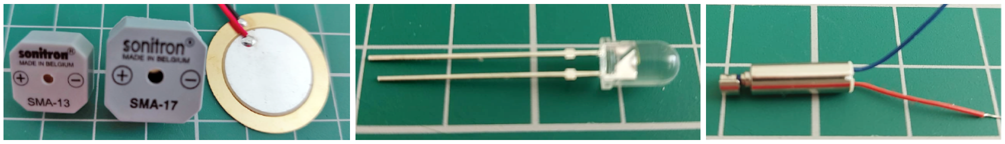

(a) (b) (c)

Figure 3: We implemented *UltraPower* prototypes using: (a) active buzzers and a passive piezo; (b) LEDs; and (c) micro-motors.

(avoiding the need of a rectifier). This simplifies the receiver, but yields less light intensity and less control over output, i.e., a LED with a rectifier will receive two times more power.

4 TECHNICAL EVALUATION

This section describes multiple evaluations caried out to characterise the technical performance of *UltraPower*. We first investigate the relationship between focal point pressure and received power, as well as distance and received power, in order to give insights into how much power can be received from an ultrasound focal point. We then analyse the feasibility of distributing power amongst several focal points to allow multiple devices to be powered independently. Next, we measure the receiver impedance to understand its efficiency and we characterised the performance of the selected output components under different levels of focal point pressure. Finally, we consolidate our findings to determine the interaction range of our *UltraPower* prototypes.

4.1 Received Power vs Focal Point Pressure

We begin our technical evaluation by investigating the relationship between focal point pressure and received power. Understanding this relationship provides insight into how much power can be transferred to a target receiver for a given focal point pressure. To that end, we created a receiving circuit for evaluation using a Manorshi MSO-P1040H07R transducer (see Table 1) and a rectifier circuit (see Figure 2). We measured the voltage output from the receiver apparatus at a fixed distance of 10cm above the centre of the transmitting ultrasound array. At this distance, the array can generate 3000Pa of sound pressure at a single focal point at maximal intensity (i.e., focal point intensity of 100%). Measurements were taken in 10% intensity increments between 0 and 100%, with no resistance applied to the load circuit.

The results of this study are shown in Figure 4 where we observe an almost linear relationship between amplitude and received voltage, matching expectations about transducer behaviour. A linear regression shows that $V \approx 0.0007152 \times P_i + 0.0581818$. This can help predict the transmitted power when the focal point pressure P_i is known; software like HandyBeam [16] or Ultraino [43] can be used to simulate pressure for different conditions. This experiment characterises the power transduced from a focal point using our *UltraPower* implementation. In practice, the load circuit will affect how much power can be delivered to the output components and is discussed in the following sections.

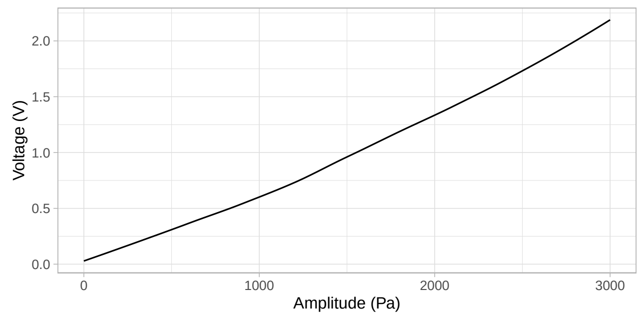

Figure 4: Measurement results showing the relationship between focal point pressure and received voltage.

4.2 Received Power vs Receiver Distance

We next investigate the amount of power that can be transferred to a receiving circuit, and the relationship between received power and the distance between transmitter and receiver. We used the earlier described test receiver with a load circuit consisting of one resistor as a generalised representation of an output component that would be driven by the receiver. Seven resistor loads were tested, giving a range of resistances that represents a variety of output components.

For each resistor load, we measured the output voltage and current , allowing us to calculate power using $P = V \times I$. The voltage was measured between the receiver and the resistor and the current was measured in the resistance by a multimeter. All of these measurements and calculations were taken in 5cm increments, between 10 and 30cm above the centre of the ultrasound transmitting array. The focal point was generated at each position using the maximum output intensity. Repeated measurements were taken for each resistance and distance and were then averaged.

Figure 5 shows the results of this experiment. A linear inverse relationship between distance and received power is observed, representing the constant dispersion of sound pressure as distance increases. We know from the previous results that voltage decreases as pressure decreases, and we know that pressure attenuates as distance increases, which is reflected in these results. These measurements characterise in a practical way the power that can be transferred to an interactive device, ranging from around 35 mW at 10 cm to 10 mW at 30 cm. It is also observed that the optimal load resistance for the proposed system is approximately 270 ohms.

The end-to-end WPT efficiency of our apparatus can thus be calculated as the ratio between power out and power in. At maximum strength, the array can consume up to 50 W, calculated using the

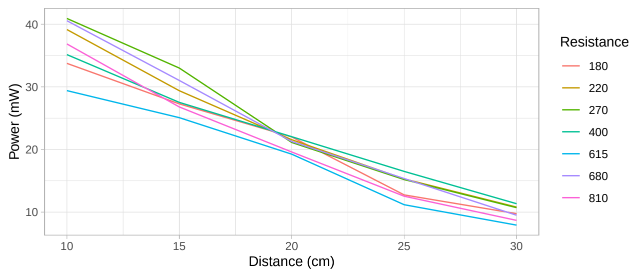

Figure 5: Relationship between receiver distance and power consumption for different resistive loads.

current consumed by 256 transducers (approx 2.5 A) multiplied by the driver voltage of 20 V. From Figure 5, we have that a circuit load of 270 ohms resistance is driven at 42 mW by a single focal point at 10 cm, thus giving an efficiency of 0.084%. This efficiency can be increased, possibly more than doubled, when using multiple focal points multiplexed in time (discussed in subsequent section) or by having a more efficient energy harvesting circuit composed of multiple receiving transducers.

4.3 Individually-Adjusted Focal Point Pressure

An array of ultrasound transducers can create multiple simultaneous focal points in mid-air, allowing us to target various independent receivers simultaneously. Distributing pressure equally amongst focal points will be inefficient if their devices have different power requirements. It is thus desirable to be able to control the amplitude targeted at each receiver to optimise power demands. For example, an interactive tangible object containing LEDs for visual feedback and a rotational motor for haptic feedback would need more pressure directed towards the motor as it requires more power than the LEDs. To demonstrate the feasibility of creating multiple focal points with individually-adjusted pressures we first employ simulations implemented using *HandyBeam* [16] — a software toolkit for ultrasound field simulations based on phased-array focusing techniques. Exemplary results are shown in Figure 6. Note from the colour scales in (c) and (d), in particular, that significantly greater pressure is obtainable in a focal point when the other points are reduced. The colored plane at $z = 0$ indicates the emission phase of each transducer used to generate the acoustic pressure fields at $z = 20$ cm.

4.4 Receiver Impedance

An incoming sound pressure wave may encounter acoustic impedance mismatches at the receiver, causing part of the pressure wave to reflect away. The impedance of the receiving transducer is therefore important, affecting the efficiency of an *UltraPower* system. To measure the impedance of the MSO-P1040H07R receiver transducers using a Keysight Impedance Analyser (E4990A). Figure 7 shows the results, modelling the relationship between operational frequency and input electrical impedance. The minimum and maximum impedance values correspond to resonance and anti-resonance, respectively. We observe a slight mismatch between resonance frequency (38.5 kHz) and transmission frequency (40 kHz). The impedance present at 40 kHz indicates potential for efficiency improvement through different transducer choice in the future. Impedance should therefore be considered alongside transducer sensitivity, discussed earlier, when assembling an *UltraPower* device.

4.5 Output Components

We investigated the behaviour of three common output components (a buzzer, a micro-motor, and an LED) in a receiving circuit, under varying levels of focal point pressure (from 0 to 3000 Pa). Our goals were to demonstrate the actuation capabilities of output components for an *UltraPower* device and investigate the feasibility of deliberately varying their output to produce varying levels of haptic feedback from a motor, or varying levels of brightness from an LED. This also helps to understand better the relationship between focal point pressure and component performance.

4.5.1 Buzzers. A microphone was used to measure the audio spectrum generated by a Sonitron SMA-17 active buzzer when powered by varying focal point intensities. The buzzer was connected to the test receiver apparatus used in the previous experiments. Figure 8a and 8b show the results of this experiment. We observe that the loudness of the buzzer can be successfully modulated by the pressure generated by the focal point, and that the minimum activation pressure is about 900 Pa.

4.5.2 Motors. We measured the rotation speed of a motor since this is an important requirement for a large set of applications, e.g., for locomotion, haptic feedback or physical actuation. We used the Back Electromotive Force (EMF) to measure the motor speed, expressed as: $E_b = V_t - I_a R_a$ (where I_a is armature current, V_t is the terminal voltage and R_a is the armature resistance). The relationship between Back EMF and motor RPM (revolutions per minute, i.e., motor speed) is expressed as $RPM = E_b * K_v$, where K_v is the motor velocity constant, measured in revolutions per minute per volt. As shown in Figure 8c the minimum pressure to activate the motor is around 1800 Pa, and the maximum motor speed achieved was 3500 rpm.

4.5.3 LEDs. We measured the brightness of an LED and its relationship with respect to the focal point pressure intensity. We used a Light Dependent Resistor (LDR) sensor placed at 5 mm from the wirelessly powered LED attached to our receiver apparatus. The resistance change was measured using an Arduino Ohmmeter, i.e., indirectly measuring the LED's brightness. The relationship between the acoustic pressure at the focal point and the LDR voltage output is shown in Figure 8d. As expected, the brightness of the emitted light is proportional to the amplitude of the focal point, while the minimum activation pressure was 600 Pa.

4.6 Component Interaction Range

Finally, we derive the range over which these components can be activated (i.e., where they can receive sufficient operational power from our output array). To that end, we simulated the maximum focal point pressure that can be produced at each point in space above the UHEV1 array across an 80x80x120 cm volume. Figure 9 shows the peak pressure distribution that can be achieved by a focal point along the $y = 0$ cm plane. It can be assumed that the pressure field is axisymmetric about the z axis. We can see that the

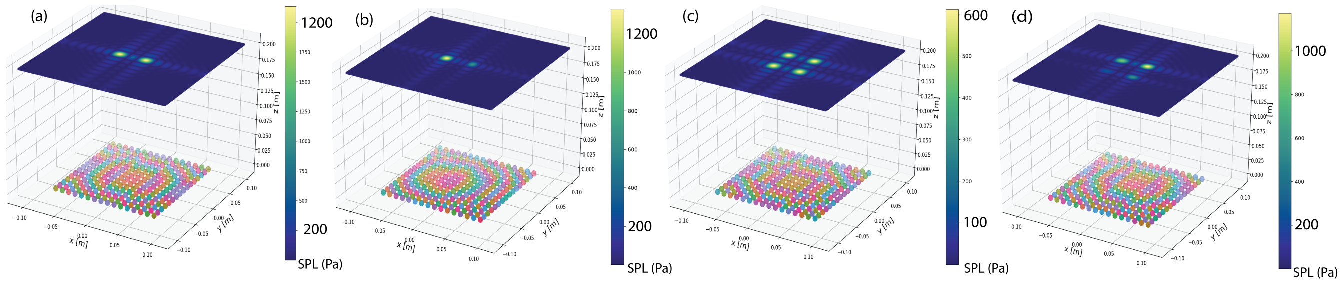

Figure 6: Acoustic pressure distribution demonstrating multiple focal points with individually-adjusted pressure. Brighter colours indicate greater sound pressure. (a): two points with equally weighted pressure ($F_1 = 1, F_2 = 1$); (b): two points with different weights ($F_1 = 1, F_2 = 0.5$); (c): four points with equally weighted pressure ($F_1 = 1, F_2 = 1, F_3 = 1, F_4 = 1$); (d): four points with different weights ($F_1 = 1, F_2 = 0.75, F_3 = 0.5, F_4 = 0.25$).

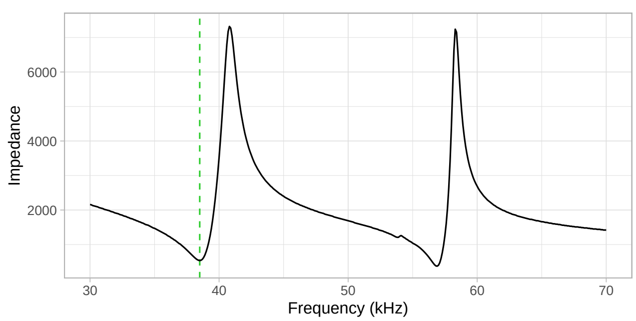

Figure 7: Impedance analysis results for the receiver transducer. Dashed line highlights the resonance frequency at 38.5 kHz**.**

highest achievable pressure density is located directly above the array, peaking around 10 cm and attenuating more rapidly beyond 50 cm. This figure also shows that pressure produced outside of the array boundaries (recall the array width is 16 cm) can activate some components. This shows that *UltraPower* is not restricted to focusing regions directly above the array .

Using the relationships between simulated acoustic pressure, rectified power, and individual component measurements (as in Figure 8), we can determine the interaction range for each component. The dotted lines in Figure 9 show the functional interaction area for the motor, buzzer and LED. Their maximum activation distances above the middle of the array are 38 cm, 79 cm and 113 cm, respectively. We can further calculate the interaction volume for each component by approximating the interaction space shown in Figure 9 by an ellipsoid, obtaining 0.008 m^3, 0.088 m^3, 0.342 m^3, respectively. Since the LED only requires 600 Pa for activation, it can be used to deliver visual feedback over 1 m above an ultrasound array, within an ellipsoid-shaped interaction volume. Note that brightness will vary over this distance, due to the relationship between relative brightness and sound pressure (Figure 8d). The buzzer has a smaller interaction volume and, like the LED will have varying performance within this space. The motor has the smallest interaction volume, however, since the energy density is so high within this region (Figure 9), its performance will be consistent, unless the user intentionally reduces the focal point pressure. The interaction volume of other components and sensors requiring different minimum operating power can be calculated in a similar way.

5 PROTOTYPE APPLICATIONS

Our technical evaluations have characterised the performance of our *UltraPower* implementation and demonstrated the feasibility of wirelessly driving a variety of output components in a controlled manner. To further showcase the potential of ultrasonic WPT for novel interactive devices, we now describe several demonstrator prototypes (see Figure 10) that explore the *UltraPower* HCI design space.

5.1 UltraPower Tangible User Interfaces

5.1.1 Turning passive into active objects. *UltraPower* can be used to add active output capabilities to passive objects, allowing dynamic physical icons without the need for an integrated power source. This can even be done *post hoc*, to add interactive capabilities to existing physical objects. To demonstrate this, we used *UltraPower* to add multimodal output to a 3D-printed rabbit, via a buzzer placed around its neck and LED placed on its head (Figure 10a). A blinking light is used to signal that an e-mail has been received; if it has high priority, the buzzer will be activated as well.

5.1.2 Active tabletop tangibles. We developed an interactive tabletop surface that uses *UltraPower* to both deliver ultrasound haptic feedback to users and wirelessly power tangible objects on its surface (Figure 10b). We used a black woven fabric that is acoustically-transparent to create an interaction surface of 30x30 cm. An ultrasound array was placed 10 cm below the centre of the surface. A Leap Motion Controller was used to track interactions, so that focal points could be targeted at users' hands (for haptic feedback) and tangible tokens (for power). We developed a set of modular tangible tokens with 2×2 and 3×3 receiver transducers, with different colour LEDs, buzzers and a micromotor. When a focal point targets one of these tokens, its LEDs are illuminated, its buzzer will emit sound, or its motor will vibrate for haptic feedback.

5.1.3 Tangible 3D displays. We created a prototype that demonstrates the use of *UltraPower* to activate the 'pixels' in a 3D digital

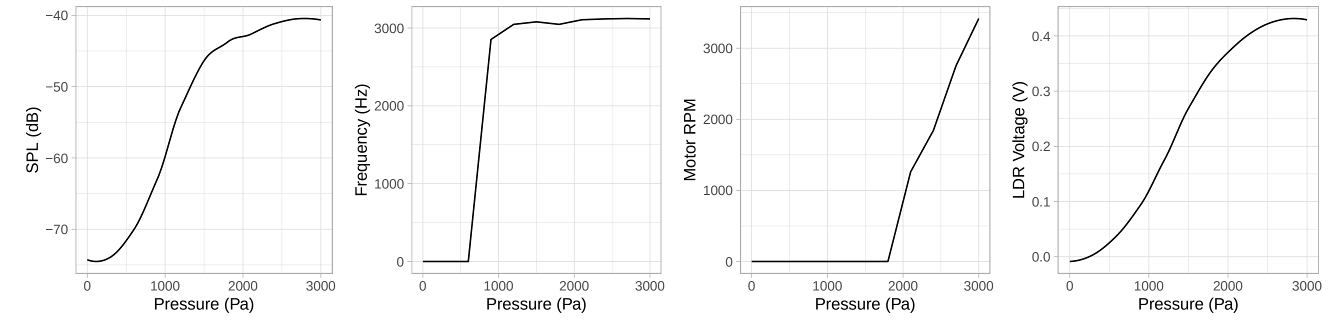

Figure 8: Behaviour of output components under varying levels of sound pressure at a focal point generated 15 cm above the transmitting array. (a) and (b) show the output spectrum of the activated buzzer, (c) shows the RPMs of the motor, and (d) shows the LED relative brightness.

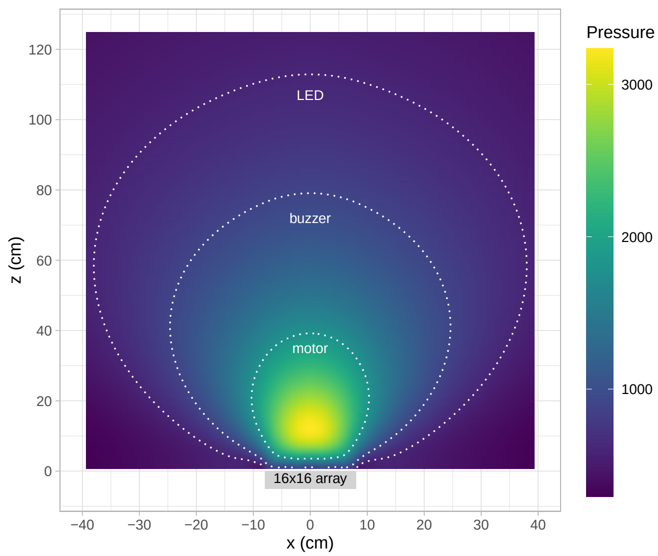

Figure 9: Simulation of focal point pressure distribution around a 256 ultrasound transducer phased array. Based on the previous experiments, we have added dotted lines that indicate the activation regions for the motor, buzzer and LED. Shaded area below $z = 0$ shows the ultrasound array width.

display (Figure 10c). LEDs with a receiver transducer were suspended above an ultrasound array using a piece of string. Since focal points can be precisely targeted at 3D positions, it is possible to selectively activate these LED pixels. To demonstrate its potential for interactivity, we used the Leap Motion Controller to enable users to activate pixels by pointing at them, causing them to flash. Moreover, since the display pixels have a physical embodiment, users can also reach into the display and directly touch them, which could enable novel interactions with the display (like miniature *Bloxels* [37] in mid-air).

5.1.4 Ambient display objects. We created a multisensory ambient information display, inspired by Ishii's *ambientROOM* [31]. A small oscillating fan driven by a micro-motor is placed near an ultrasound transmitting phased array device. The fan spins when a notification is received (similar to a *Pinwheel* [30]). Users can interrupt the ambient display by placing their hand between the ultrasound emitter and the fan's receiving circuit, without the need for additional sensors. Since 40 kHz ultrasound is almost completely reflected by the skin, the hand will block any acoustic pressure from reaching the rectifying receiver, thus stopping the fan (as in Figure 10d). In this instance, ultrasonic mid-air haptic information can be used to provide information about the notification in a non-visual way; e.g., *UltraPower* delivers power to the fan but modulating the intensity with a pulse so that the user feels it when blocking the reception. The pulsing haptics indicates the importance of the message or its reception time. This demonstrates the use of an ultrasound wave to both power a proximal component and produce mid-air haptic feedback, using the same signal.

5.2 UltraPower Wearable Devices

UltraPower can be integrated into wearable devices with a variety of form factors. Rings and bracelets are the most suitable for *UltraPower* since they are worn on the hand, which can be targeted during gesture interaction (or hands-on interaction with our tabletop system described earlier). Moreover, unlike self-powered wearables that can support μW functionalities like sensing and short range wireless transmissions [40], with *UltraPower* we can also support additional functionalities with greater power demands such as audible, visual, and tactile feedback.

5.2.1 Haptic ring. We built a wearable accessory that applies vibration feedback on the back of the hand when the receiving circuit placed inside a ring is targeted by a focal point. In Figure 10e, the user wears the receiver on their finger and the vibration motor on the back of the hand. The hand can be tracked with a Leap Motion Controller, so that the ultrasound array can focus its energy on the receiver as the hand moves above the device. This approach enables a combination of haptic sensations on both sides of the hand without the need to wear gloves or more complex devices.

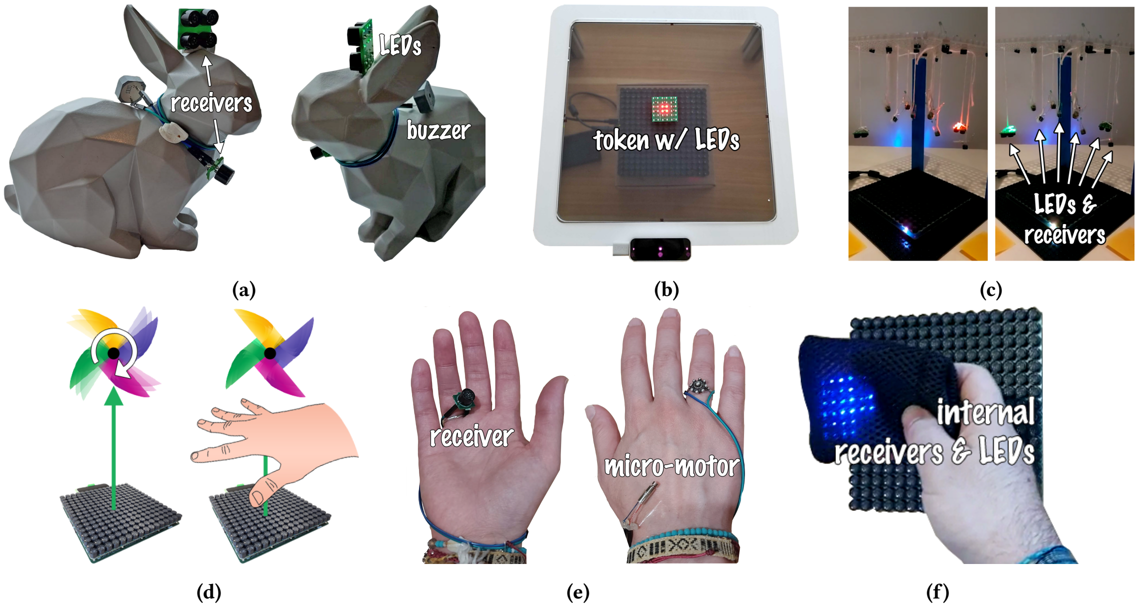

Figure 10: Tangible *UltraPower* prototypes: (a) active physical objects; (b) tabletop tangible tokens; (c) physical 3D display pixels; (d) ambient fan display with haptic information; (e) wearable device for haptic feedback; (f) fabric bag with integrated electronics.

Traditional mid-air ultrasonic haptics can only target the fingertips and the palm, but with *UltraPower* a wearable ring can produce tactile sensation on the back of the hand at the same time.

5.2.2 Interactive jewellery, clothing and materials. Our final demonstrator application illustrates how *UltraPower* can be used to power electronic components integrated with fabrics and materials. In Figure 10f, ultrasound passes through the material of a small bag, providing power to an internal receiver and LED grid (one of the LED tokens from the tabletop system). This shows the potential to deliver power to (and through) clothing and accessories, e.g., for presenting notifications [81] or as a means of self expression and display [18]. This is possible with *UltraPower* since LEDs can be activated over 1 m from an emitter, with only limited amplitude loss when passing through fabrics [20].

6 DISCUSSION AND FUTURE WORK

This work has demonstrated the feasibility of powering untethered interactive devices using ultrasound. Our implementation and *UltraPower* prototypes have exemplified a range of interactions that can be powered in this way. There are, however, technical limitations to this WPT method which determine the situations where *UltraPower* is currently most appropriate for use and provide compelling challenges for future research. Moreover, the fact that ultrasound is much less regulated by governments and other regulatory bodies, unlike the electromagnetic spectrum (used by other WPT methods), presents flexible opportunities for its exploitation—which we hope inspires others to build on this work.

One limitation of *UltraPower* is the effective range of operation (best shown by Figure 9). Output components can only be activated if the targeted focal point has sufficient energy. For our ultrasound array with 256 transducers, this meant components needed to be within 1.2 m, with those that consume more power (e.g., motors) needing to be even closer. A larger and more powerful ultrasound array would increase the range of operation; e.g., others are investigating haptic applications of much larger arrays (e.g., 2241 [68] and 3984 emitters [29]) which would improve the effective range of interaction significantly. Using lower ultrasonic frequencies to reduce attenuation would also increase range.

While *UltraPower* targets receivers in 3D space, currently it does not explicitly include the tracking of position and orientation of the receivers. The orientation of a receiving transducer affects power transfer significantly: e.g., losing 90% of energy at 67°relative to the array. Similarly, if the emitter array is not correctly focusing onto the receiver then the harvested power reduces by more than 90%. A variety of options are available to track the receiver, including hand trackers like the Leap Motion controller for targeting devices worn on the fingers or wrist, and optical sensors for tangible marked objects (e.g., using the LeapUVC API). The Leap Motion controller has a high refresh rate and its tracking is stable with fingertip estimation errors of 4–5mm [75]. We thus expect, and indeed have observed through our prototypes, that *UltraPower* can robustly support dynamic and mobile HCI applications using off-the-shelf tracking technologies.

Finally, 3D printed acoustic metamaterials [64] could be used along with the transmitting array to create additional or more exotic pressure fields thus enabling a more efficient spatial distribution of *UltraPower* as well as the possibility of powering devices that do not have a direct line of sight path with the ultrasound source. Note that analogous techniques have been proposed in 5G and 6G wireless radio communications [62].

Despite the range limitation, we have demonstrated that *UltraPower* is well suited for mid-range proximal interactions near a desktop or large surface. Namely, we created a range of tangible device prototypes as this is a compelling interaction scenario that matches the operational characteristics of ultrasonic WPT. While interactive surfaces with integrated ultrasound arrays for haptics have been previously explored [8], we think that the same form factor could utilise *UltraPower* to further enable novel tabletop tangible interfaces, with flexible device designs capable of providing audio, haptic and visual feedback. Moreover, *UltraPower* could also support novel 3D interactions in mid-air, above the desktop surface, as the tangible devices would still receive power when lifted from the table.

For an interactive object to receive power, ultrasound needs to be focused towards the position of its receiver transducer/s, requiring knowledge of its position and orientation. Optimal tracking was out of the scope of this paper, but tracking can be achieved using optical sensors, IR proximity or ultrasonic SONAR techniques, for example. Tracking of distance does not need to be highly precise if the receiver is pointed towards the array, as sound pressure is distributed along an elongated ellipsoid (rather than a focal 'point'), several wavelengths long and perpendicular to the sound beam direction, thus allowing activation in poor determination of distance if necessary. This approach could be useful in games or educational applications by only activating feedback when a user holds an object in the correct place, or moves along the correct trajectory (*a la* the 'buzz wire' game [55]).

A better understanding of the types of sensors and actuators that can be powered by *UltraPower* is needed. This research took a formative look at simple components that can be used to create multisensory user experiences in an HCI context, however there are many more complex components that we have not yet studied. For example, Bluetooth modules, IMUs, GPS circuits and other connectivity devices offer great potential for more complicated interactions (both with users and other computing devices). The analysis presented in Section 4 can aid in understanding what other components could be remotely activated and powered by *UltraPower* as well as what modifications would be needed.

Our technical evaluation focused on output components for delivering feedback to users. However, *UltraPower* can also be used to power input components, allowing the creation of interactive objects that can sense a user's actions. Push buttons like the C&K K12 series, for example, require only 0.2 mW power to detect activation; for comparison, over 20 mW can be received 20 cm above our prototype (Figure 5). For detected actions like a button press to have an effect on an interactive system, it would be necessary to detect when they occur. This could be achieved using low-powered components: e.g., an infrared LED flash could be detected by the optical tracking system. Future research could investigate the novel input possibilities enabled by *UltraPower* and suitable methods for sensing them.

Finally, research could investigate new interaction techniques with *UltraPower* applications. We see mid-air haptic feedback combined with *UltraPower* actuated components as an exciting new area, utilising the intended functionality of a haptics array but extending it with additional feedback possibilities (e.g., tactile feedback on the back of the hand from a wearable). We hope our initial approach and prototypes will encourage other researchers, designers, and educators to explore a range of new applications, and will enable further evaluation of its potential for interactive computing.

7 CONCLUSION

In this work we investigated WPT using focused ultrasound for HCI applications — a concept we call *UltraPower*. We demonstrated how *UltraPower* can be used to power multiple small interactive devices even through fabric in a robust and precisely targeted wireless manner. We discussed an implementation that uses low-cost electronic components and a standard ultrasound emitter array already widely used in HCI research for haptic feedback. Through a detailed technical evaluation we characterised the performance of our *UltraPower* implementation and demonstrated its ability to selectively and accurately transfer power to distant interactive objects, even those over 1 m away. Further, this formative exploration of *UltraPower* focused on its use for tangible and wearable interaction and their respective design space, as these are compelling use cases that are well suited to the operating characteristics of an *UltraPower* system. To show how *UltraPower*'s unique capabilities can be utilised we developed several prototype demonstrators, including a tabletop tangible interface that supports off-surface interaction and a 3D display with physical pixels. Wireless power transfer capabilities can support rapid prototyping of novel devices like these, enable designers to explore new and more flexible form factors for tangible objects, and lead to new interaction techniques through the provision of power through the air. Using the fundamental principles described herein, we encourage novel and expert tangible designers to exploit the capabilities of *UltraPower* and to create novel interactive devices in new application areas.

ACKNOWLEDGMENTS

This project has received funding from the European Union's Horizon 2020 research and innovation programme under grant agreement No 737087, Levitate. Orestis G. would also like to acknowledge funding from the Marie Skłodowska-Curie project NEWSENs, No 787180. Asier M. has been funded by Government of Navarre (FEDER) 0011-1365-2019-000086.

REFERENCES

[1] Kush Agarwal, Rangarajan Jegadeesan, Yong-Xin Guo, and Nitish V Thakor. 2017. Wireless power transfer strategies for implantable bioelectronics. *IEEE Reviews in Biomedical Engineering* 10 (2017), 136–161.

[2] Johnson I Agbinya. 2015. *Wireless power transfer*. Vol. 45. River Publishers.

[3] Carl Andersson and Jens Ahrens. 2017. *Database of Ultrasonic Transducer Radiation Characteristics*. https://doi.org/10.5281/zenodo.1118386

[4] Daniel Ashbrook, Patrick Baudisch, and Sean White. 2011. Nenya: Subtle and Eyes-Free Mobile Input with a Magnetically-Tracked Finger Ring. In *Proceedings of the SIGCHI Conference on Human Factors in Computing Systems - CHI '11*. ACM Press, 2043–2046. https://doi.org/10.1145/1978942.1979238

[5] Andrea Bianchi, Ian Oakley, Jong Keun Lee, Dong Soo Kwon, and Vassilis Kostakos. 2011. Haptics for Tangible Interaction: A Vibro-Tactile Prototype. In *Proceedings of the fifth international conference on Tangible, embedded, and embodied interaction - TEI '11*. ACM Press, 283–284. https://doi.org/10.1145/1935701.1935764

[6] Anne-Claire Bourland, Peter Gorman, Jess McIntosh, and Asier Marzo. 2018. Project telepathy. *interactions* 25, 5 (2018), 16–17.

[7] Samuele Carcagno, Andrew Di Battista, and Christopher J Plack. 2019. Effects of High-Intensity Airborne Ultrasound Exposure on Behavioural and Electrophysiological Measures of Auditory Function. *Acta Acustica united with Acustica* 105, 6 (2019), 1183–1197.

[8] Thomas Carter, Sue Ann Seah, Benjamin Long, Bruce Drinkwater, and Sriram Subramanian. 2013. UltraHaptics: Multi-Point Mid-Air Haptic Feedback for Touch Surfaces. In *Proceedings of the 26th Symposium on User Interface Software and Technology - UIST '13*. ACM Press, 505–514. https://doi.org/10.1145/2501988.2502018

[9] Jayant Charthad, Nemat Dolatsha, Angad Rekhi, and Amin Arbabian. 2016. System-level analysis of far-field radio frequency power delivery for mm-sized sensor nodes. *IEEE Transactions on Circuits and Systems I: Regular Papers* 63, 2 (2016), 300–311.

[10] Christopher Chen, David Howard, Steven L. Zhang, Youngwook Do, Sienna Sun, Tingyu Cheng, Zhong Lin Wang, Gregory D. Abowd, and HyunJoo Oh. 2020. SPIN (Self-powered Paper Interfaces): Bridging Triboelectric Nanogenerator with Folding Paper Creases. In *Proceedings of the 14th International Conference on Tangible, Embedded, and Embodied Interaction - TEI '20*. ACM Press, 431–442. https://doi.org/10.1145/3374920.3374946

[11] Christian Cherek, David Asselborn, Simon Voelker, and Jan Borchers. 2019. Off-Surface Tangibles: Exploring the Design Space of Midair Tangible Interaction. In *Extended Abstracts of the 2019 CHI Conference on Human Factors in Computing Systems - CHI EA '19*. ACM Press, LBW 2115. https://doi.org/10.1145/3290607.3312966

[12] Artem Dementyev, Hsin-Liu Kao, Inrak Choi, Deborah Ajilo, Maggie Xu, Joseph A Paradiso, Chris Schmandt, and Sean Follmer. 2016. Rovables: Miniature on-body robots as mobile wearables. In *Proceedings of the 29th Annual Symposium on User Interface Software and Technology*. 111–120.

[13] Lokesh Dhakar. 2017. Overview of energy harvesting technologies. In *Triboelectric Devices for Power Generation and Self-Powered Sensing Applications*. Springer, 9–37.

[14] Andrew Di Battista. 2019. The effect of 40 kHz ultrasonic noise exposure on human hearing. *Proceedings of the 23rd International Congress on Acoustics - ICA '19* (2019), 4783–4788.

[15] Julie Ducasse, Marc Macé, Bernard Oriola, and Christophe Jouffrais. 2018. BotMap: Non-Visual Panning and Zooming with an Actuated Tabletop Tangible Interface. *ACM Transactions on Computer-Human Interaction* 25, 4 (2018), Article 24. https://doi.org/10.1145/3204460

[16] Jerzy Dziewierz. 2019. HandyBeam. https://github.com/ultraleap/HandyBeam.

[17] Xiaoran Fan, Han Ding, Sugang Li, Michael Sanzari, Yanyong Zhang, Wade Trappe, Zhu Han, and Richard E. Howard. 2018. Energy-Ball: Wireless Power Transfer for Batteryless Internet of Things through Distributed Beamforming. *Proceedings of the ACM on Interactive, Mobile, Wearable and Ubiquitous Technologies* 2, 2 (2018), 1–22. https://doi.org/10.1145/3214268

[18] Jutta Fortmann, Erika Root, Susanne Boll, and Wilko Heuten. 2016. Tangible Apps Bracelet: Designing Modular Wrist-Worn Digital Jewellery for Multiple Purposes. In *Proceedings of the 2016 ACM Conference on Designing Interactive Systems - DIS '16*. ACM Press, 841–852. https://doi.org/10.1145/2901790.2901838

[19] Euan Freeman, Stephen Brewster, and Vuokko Lantz. 2014. Tactile Feedback for Above-Device Gesture Interfaces: Adding Touch to Touchless Interactions. In *Proceedings of the 16th International Conference on Multimodal Interaction - ICMI '14*. ACM Press, 419–426. https://doi.org/10.1145/2663204.2663280

[20] Euan Freeman, Asier Marzo, Praxitelis B. Kourtelos, Julie R. Williamson, and Stephen Brewster. 2019. Enhancing Physical Objects with Actuated Levitating Particles. In *Proceedings of the 8th ACM International Symposium on Pervasive Displays - PerDis '19*. ACM Press, Article 24. https://doi.org/10.1145/3321335.3324939

[21] Euan Freeman, Julie Williamson, Sriram Subramanian, and Stephen Brewster. 2018. Point-and-Shake: Selecting from Levitating Object Displays. In *Proceedings of the 36th Annual ACM Conference on Human Factors in Computing Systems - CHI '18*. ACM Press, Paper 18. https://doi.org/10.1145/3173574.3173592

[22] William Frier, Damien Ablart, Jamie Chilles, Benjamin Long, Marcello Giordano, Marianna Obrist, and Sriram Subramanian. 2018. Using Spatiotemporal Modulation to Draw Tactile Patterns in Mid-air. In *Proceedings of EuroHaptics 2018*. Springer.

[23] Tatsuki Fushimi, Asier Marzo, Bruce W Drinkwater, and Thomas L Hill. 2019. Acoustophoretic volumetric displays using a fast-moving levitated particle. *Applied Physics Letters* 115, 6 (2019), 064101.

[24] Jaime Garnica, Raul A Chinga, and Jenshan Lin. 2013. Wireless power transmission: From far field to near field. *Proc. IEEE* 101, 6 (2013), 1321–1331.

[25] Orestis Georgiou, Konstantinos Mimis, David Halls, William H Thompson, and David Gibbins. 2016. How many Wi-Fi APs does it take to light a lightbulb? *IEEE Access* 4 (2016), 3732–3746.

[26] Jeremy Gummeson, Bodhi Priyantha, and Jie Liu. 2014. An energy harvesting wearable ring platform for gestureinput on surfaces. In *Proceedings of the 12th annual international conference on Mobile systems, applications, and services*. 162–175.

[27] Kyle Harrington, David R. Large, Gary Burnett, and Orestis Georgiou. 2018. Exploring the Use of Mid-Air Ultrasonic Feedback to Enhance Automotive User Interfaces. In *Proceedings of the 10th International Conference on Automotive User Interfaces and Interactive Vehicular Applications - AutomotiveUI '18*. ACM Press, 11–20. https://doi.org/10.1145/3239060.3239089

[28] Ryuji Hirayama, Diego Martinez Plasencia, Nobuyuki Masuda, and Sriram Subramanian. 2019. A volumetric display for visual, tactile and audio presentation using acoustic trapping. *Nature* 575 (2019). https://doi.org/10.1038/s41586-019-1739-5

[29] Seki Inoue, Yasutoshi Makino, and Hiroyuki Shinoda. 2015. Active touch perception produced by airborne ultrasonic haptic hologram. In *Proceedings of IEEE World Haptics Conference - WHC '15*. IEEE, 362–367. https://doi.org/10.1109/WHC.2015.7177739

[30] Hiroshi Ishii, Sandia Ren, and Phil Frei. 2001. Pinwheels: Visualizing Information Flow in an Architectural Space. In *CHI '01 Extended Abstracts on Human Factors in Computing Systems* (Seattle, Washington) *(CHI EA '01)*. Association for Computing Machinery, New York, NY, USA, 111–112. https://doi.org/10.1145/634067.634135

[31] Hiroshi Ishii, Craig Wisneski, Scott Brave, Andrew Dahley, Matt Gorbet, Brygg Ullmer, and Paul Yarin. 1998. ambientROOM: Integrating Ambient Media with Architectural Space. In *Proceedings of the SIGCHI Conference on Human Factors in Computing Systems - CHI '98*. ACM Press, 173–174. https://doi.org/10.1145/286498.286652

[32] Toshihiko Ishiyama, Yasuyuki Kanai, Junichi Ohwaki, and Masato Mino. 2003. Impact of a wireless power transmission system using an ultrasonic air transducer for low-power mobile applications. In *IEEE Symposium on Ultrasonics, 2003*, Vol. 2. IEEE, 1368–1371.

[33] Takayuki Iwamoto, Mari Tatezono, and Hiroyuki Shinoda. 2008. Non-contact method for producing tactile sensation using airborne ultrasound. In *Proceedings of EuroHaptics 2008*. Springer, 504–513. https://doi.org/10.1007/978-3-540-69057-3_64

[34] Vikram Iyer, Elyas Bayati, Rajalakshmi Nandakumar, Arka Majumdar, and Shyamnath Gollakota. 2018. Charging a Smartphone Across a Room Using Lasers. *Proceedings of the ACM on Interactive, Mobile, Wearable and Ubiquitous Technologies* 1, 4 (2018), 1–21. https://doi.org/10.1145/3161163

[35] Sergi Jordà, Günter Geiger, Marcos Alonso, and Martin Kaltenbrunner. 2007. The reacTable: Exploring the Synergy between Live Music Performance and Tabletop Tangible Interfaces. In *Proceedings of the 1st International Conference on Tangible and Embedded Interaction - TEI '07*. ACM Press, 139–146. https://doi.org/10.1145/1226969.1226998

[36] Hsin-Liu Kao, Artem Dementyev, Joseph A Paradiso, and Chris Schmandt. 2015. NailO: fingernails as an input surface. In *Proceedings of the 33rd Annual ACM Conference on Human Factors in Computing Systems*. 3015–3018.

[37] Jinha Lee, Yasuaki Kakehi, and Takeshi Naemura. 2009. Bloxels: Glowing Blocks as Volumetric Pixels. In *Proceedings of SIGGRAPH 2009 Emerging Technologies*. ACM Press, Article 5. https://doi.org/10.1145/1597956.1597961

[38] TG Leighton. 2016. Are some people suffering as a result of increasing mass exposure of the public to ultrasound in air? *Proceedings of the Royal Society A: Mathematical, Physical and Engineering Sciences* 472, 2185 (2016), 20150624.

[39] Jakob Leitner and Michael Haller. 2011. Geckos: Combining Magnets and Pressure Images to Enable New Tangible-object Design and Interaction. In *Proceedings of the SIGCHI Conference on Human Factors in Computing Systems - CHI '04*. ACM Press, 2985–2994. https://doi.org/10.1145/1978942.1979385

[40] Vladimir Leonov. 2011. Energy harvesting for self-powered wearable devices. In *Wearable monitoring systems*. Springer, 27–49.

[41] Hannah Limerick, Richard Hayden, David Beattie, Orestis Georgiou, and Jörg Müller. 2019. User Engagement for Mid-Air Haptic Interactions with Digital Signage. In *Proceedings of the 8th ACM International Symposium on Pervasive Displays - PerDis '19*. ACM Press, to appear.

[42] Benjamin Long, Sue Ann Seah, Tom Carter, and Sriram Subramanian. 2014. Rendering Volumetric Haptic Shapes in Mid-Air using Ultrasound. *ACM Transactions on Graphics* 33, 6 (2014), Article 181. https://doi.org/10.1145/2661229.2661257

[43] Asier Marzo, Tom Corkett, and Bruce W. Drinkwater. 2018. Ultraino: An Open Phased-Array System for Narrowband Airborne Ultrasound Transmission. *IEEE Transactions on Ultrasonics, Ferroelectrics, and Frequency Control* 65, 1 (2018), 102–111. https://doi.org/10.1109/TUFFC.2017.2769399

[44] Asier Marzo and Bruce W Drinkwater. 2019. Holographic acoustic tweezers. *Proceedings of the National Academy of Sciences* 116, 1 (2019), 84–89.

[45] Asier Marzo, Steven Kockaya, Euan Freeman, and Julie Williamson. 2019. Tangible Interactions with Acoustic Levitation. In *Extended Abstracts of the 2019 CHI Conference on Human Factors in Computing Systems* (Glasgow, Scotland Uk) *(CHI EA '19)*. Association for Computing Machinery, New York, NY, USA, 1–4. https://doi.org/10.1145/3290607.3313265

[46] Asier Marzo, Sue Ann Seah, Bruce W. Drinkwater, Deepak Ranjan Sahoo, Benjamin Long, and Sriram Subramanian. 2015. Holographic acoustic elements for manipulation of levitated objects. *Nature Communications* 6 (2015), Article 8661. https://doi.org/10.1038/ncomms9661

[47] Jess McIntosh, Paul Strohmeier, Jarrod Knibbe, Sebastian Boring, and Kasper Hornbæk. 2019. Magnetips: Combining Fingertip Tracking and Haptic Feedback for Around-Device Interaction. In *Proceedings of the 2019 CHI Conference on Human Factors in Computing Systems - CHI '19*. ACM Press. https://doi.org/10.1145/3290605.3300638

[48] James O McSpadden and John C Mankins. 2002. Space solar power programs and microwave wireless power transmission technology. *IEEE microwave magazine*

3, 4 (2002), 46–57.

[49] Takashi Miyaki, Yong Ding, Behnam Banitalebi, and Michael Beigl. 2011. Things that Hover: Interaction with Tiny Battery-less Robots on Desktop. In *Extended Abstracts of the 2011 CHI Conference on Human Factors in Computing Systems - CHI EA '11 (alt.chi)*. ACM Press, 531–540. https://doi.org/10.1145/1979742.1979624

[50] Kikuya Miyamura, Yuichi Miyaji, and Ren Ohmura. 2017. Feasibility study on wireless power transfer for wearable devices. In *Proceedings of the 2017 ACM International Symposium on Wearable Computers - ISWC '17*. ACM Press, 166–167. https://doi.org/10.1145/3123021.3123030

[51] Yasuaki Monnai, Keisuke Hasegawa, Masahiro Fujiwara, Kazuma Yoshino, Seki Inoue, and Hiroyuki Shinoda. 2014. HaptoMime: Mid-Air Haptic Interaction with a Floating Virtual Screen. In *Proceedings of the 27th Symposium on User Interface Software and Technology - UIST '14*. ACM Press, 663–667. https://doi.org/10.1145/2642918.2647407

[52] Rafael Morales, Asier Marzo, Sriram Subramanian, and Diego Martínez. 2019. LeviProps: Animating Levitated Optimized Fabric Structures using Holographic Acoustic Tweezers. In *Proceedings of the 32nd ACM User Interface Software and Technology Symposium - UIST '19*. ACM Press, 651–661. https://doi.org/10.1145/3332165.3347882

[53] Rafael Morales González, Caroline Appert, Gilles Bailly, and Emmanuel Pietriga. 2016. TouchTokens: Guiding Touch Patterns with Passive Tokens. In *Proceedings of the 2016 CHI Conference on Human Factors in Computing Systems* (San Jose, California, USA) *(CHI '16)*. Association for Computing Machinery, New York, NY, USA, 4189–4202. https://doi.org/10.1145/2858036.2858041

[54] Rafael Morales González, Caroline Appert, Gilles Bailly, and Emmanuel Pietriga. 2017. Passive yet Expressive TouchTokens. In *Proceedings of the 2017 CHI Conference on Human Factors in Computing Systems* (Denver, Colorado, USA) *(CHI '17)*. Association for Computing Machinery, New York, NY, USA, 3741–3745. https://doi.org/10.1145/3025453.3025894

[55] Rafael Morales González, Euan Freeman, and Orestis Georgiou. 2020. Levi-Loop: A Mid-Air Gesture Controlled Levitating Particle Game. In *Extended Abstracts of the 2020 CHI Conference on Human Factors in Computing Systems* (Honolulu, HI, USA) *(CHI EA '20)*. Association for Computing Machinery, New York, NY, USA, 1–4. https://doi.org/10.1145/3334480.3383152

[56] Kensuke Nagaya, Jiang Liu, and Shigeru Shimamoto. 2019. Design of Ultrasonic Wireless Power Transfer System. In *2019 IEEE Globecom Workshops (GC Wkshps)*. IEEE, 1–6.

[57] Diana Nowacka, Karim Ladha, Nils Y. Hammerla, Daniel Jackson, Cassim Ladha, Enrico Rukzio, and Patrick Olivier. 2013. Touchbugs: Actuated Tangibles on Multi-Touch Tables. In *Proceedings of the SIGCHI Conference on Human Factors in Computing Systems - CHI '13*. ACM Press, 759–762. https://doi.org/10.1145/2470654.2470761

[58] Yoichi Ochiai, Takayuki Hoshi, and Jun Rekimoto. 2014. Pixie Dust: Graphics Generated by Levitated and Animated Objects in Computation Acoustic-Potential Field. *ACM Transactions on Graphics* 33, 4 (2014), Article 85. https://doi.org/10.1145/2601097.2601118

[59] Yoichi Ochiai, Takayuki Hoshi, and Ippei Suzuki. 2017. Holographic whisper: Rendering audible sound spots in three-dimensional space by focusing ultrasonic waves. In *Proceedings of the 2017 CHI Conference on Human Factors in Computing Systems*. 4314–4325.

[60] Masa Ogata and Masaaki Fukumoto. 2015. FluxPaper: Reinventing Paper with Dynamic Actuation Powered by Magnetic Flux. In *Proceedings of the SIGCHI Conference on Human Factors in Computing Systems - CHI '15*. ACM Press, 29–38. https://doi.org/10.1145/2702123.2702516

[61] Themis Omirou, Asier Marzo, Sue Ann Seah, and Sriram Subramanian. 2015. LeviPath: Modular Acoustic Levitation for 3D Path Visualisations. In *Proceedings of the 33rd Annual ACM Conference on Human Factors in Computing Systems - CHI '15*. ACM Press, 309–312. https://doi.org/10.1145/2702123.2702333

[62] Cunhua Pan, Hong Ren, Kezhi Wang, Maged Elkashlan, Arumugam Nallanathan, Jiangzhou Wang, and Lajos Hanzo. 2020. Intelligent reflecting surface aided MIMO broadcasting for simultaneous wireless information and power transfer. *IEEE Journal on Selected Areas in Communications* (2020).

[63] Esben Warming Pedersen and Kasper Hornbæk. 2011. Tangible Bots: Interaction with Active Tangibles in Tabletop Interfaces. In *Proceedings of the 2011 annual conference on Human factors in computing systems - CHI '11*. ACM Press, 2975–2984. https://doi.org/10.1145/1978942.1979384

[64] Spyros Polychronopoulos and Gianluca Memoli. 2020. Acoustic levitation with optimized reflective metamaterials. *Scientific reports* 10, 1 (2020), 1–10.

[65] Shashank Priya, Hyun-Cheol Song, Yuan Zhou, Ronnie Varghese, Anuj Chopra, Sang-Gook Kim, Isaku Kanno, Liao Wu, Dong Sam Ha, Jungho Ryu, et al. 2019. A review on piezoelectric energy harvesting: materials, methods, and circuits. *Energy Harvesting and Systems* 4, 1 (2019), 3–39.

[66] Angad S Rekhi, Butrus T Khuri-Yakub, and Amin Arbabian. 2017. Wireless power transfer to millimeter-sized nodes using airborne ultrasound. *IEEE transactions on ultrasonics, ferroelectrics, and frequency control* 64, 10 (2017), 1526–1541.

[67] Qiongfeng Shi, Tao Wang, and Chengkuo Lee. 2016. MEMS based broadband piezoelectric ultrasonic energy harvester (PUEH) for enabling self-powered implantable biomedical devices. *Scientific reports* 6 (2016), 24946.

[68] Shun Suzuki, Keisuke Hasegawa, Yasutoshi Makino, and Shinoda. 2018. Haptic Tracing of Midair Linear Trajectories Presented by Ultrasound Bessel Beams. In *Proceedings of EuroHaptics 2018 in LNCS 10893 - EuroHaptics '18*. Springer International Publishing, 209–220. https://doi.org/10.1007/978-3-319-93445-7_19

[69] Rajesh V Taalla, Md Shamsul Arefin, Akif Kaynak, and Abbas Z Kouzani. 2018. A review on miniaturized ultrasonic wireless power transfer to implantable medical devices. *IEEE Access* 7 (2018), 2092–2106.

[70] Ryoko Takahashi, Keisuke Hasegawa, and Hiroyuki Shinoda. 2018. Lateral Modulation of Midair Ultrasound Focus for Intensified Vibrotactile Stimuli. In *Proceedings of EuroHaptics 2018 in LNCS 10894 - EuroHaptics '18*. Springer International Publishing, 276–288. https://doi.org/10.1007/978-3-319-93399-3_25

[71] Ryo Takahashi, Takuya Sasatani, Fuminori Okuya, Yoshiaki Narusue, and Yoshihiro Kawahara. 2018. A Cuttable Wireless Power Transfer Sheet. *Proceedings of the ACM on Interactive, Mobile, Wearable and Ubiquitous Technologies* 2, 4 (2018), 1–25. https://doi.org/10.1145/3287068

[72] Hsin-Ruey Tsai, Min-Chieh Hsiu, Jui-Chun Hsiao, Lee-Ting Huang, Mike Chen, and Yi-Ping Hung. 2016. TouchRing: subtle and always-available input using a multi-touch ring. In *Proceedings of the 18th International Conference on Human-Computer Interaction with Mobile Devices and Services Adjunct - MobileHCI '16*. ACM Press, 891–898. https://doi.org/10.1145/2957265.2961860

[73] Victor Farm-Guoo Tseng, Sarah S Bedair, and Nathan Lazarus. 2017. Acoustic wireless power transfer with receiver array for enhanced performance. In *2017 IEEE Wireless Power Transfer Conference (WPTC)*. IEEE, 1–4.

[74] Victor Farm-Guoo Tseng, Sarah S Bedair, and Nathan Lazarus. 2017. Phased array focusing for acoustic wireless power transfer. *IEEE transactions on ultrasonics, ferroelectrics, and frequency control* 65, 1 (2017), 39–49.

[75] Pier Paolo Valentini and Eugenio Pezzuti. 2017. Accuracy in fingertip tracking using Leap Motion Controller for interactive virtual applications. *International Journal on Interactive Design and Manufacturing (IJIDeM)* 11, 3 (2017), 641–650.

[76] Jan B. F. van Erp, Alexander Toet, Koos Meijer, Joris B. Janssen, and Arnoud de Jong. 2015. Subjective User Experience and Performance with Active Tangibles on a Tabletop Interface. In *Proceedings of the International Conference on Distributed, Ambient, and Pervasive Interactions in LNCS 9189 - DAPI '15*. Springer International Publishing, 212–223. https://doi.org/10.1007/978-3-319-20804-6

[77] Nicolas Villar, Daniel Cletheroe, Greg Saul, Christian Holz, Tim Regan, Oscar Salandin, Misha Sra, Hui-Shyong Yeo, William Field, and Haiyan Zhang. 2018. Project zanzibar: A portable and flexible tangible interaction platform. In *Proceedings of the 2018 CHI Conference on Human Factors in Computing Systems*. 1–13.

[78] Edward J. Wang, Manuja Sharma, Yiran Zhao, and Shwetak N. Patel. 2018. CASPER: Capacitive serendipitous power transfer for through-body charging of multiple wearable devices. In *Proceedings of the 2018 ACM International Symposium on Wearable Computers - ISWC '18*. ACM Press, 188–195. https://doi.org/10.1145/3267242.3267254

[79] Malte Weiss, Florian Schwarz, Simon Jakubowski, and Jan Borchers. 2010. Madgets: Actuating Widgets on Interactive Tabletops. In *Proceedings of the 23rd Annual ACM Symposium on User Interface Software and Technology - UIST '10*. ACM Press, 293–302. https://doi.org/10.1145/1866029.1866075

[80] Paul Worgan, Jarrod Knibbe, Mike Fraser, and Diego Martinez Plasencia. 2016. PowerShake: Power Transfer interactions for mobile devices. In *Proceedings of the SIGCHI Conference on Human Factors in Computing Systems - CHI '16*. ACM Press, 4734–4745. https://doi.org/10.1145/2858036.2858569

[81] Cheng Xu and Kent Lyons. 2015. Shimmering Smartwatches: Exploring the Smartwatch Design Space. In *Proceedings of the 9th International Conference on Tangible, Embedded, and Embodied Interaction - TEI '15*. ACM Press, 69–76. https://doi.org/10.1145/2677199.2680599

[82] Thoriq Zaid, Shakir Saat, and Norezmi Jamal. 2014. A development of low-power acoustic energy transfer system using push-pull power converter. (2014).

[83] Yang Zhang, Yasha Iravantchi, Haojian Jin, Swarun Kumar, and Chris Harrison. 2019. Sozu: Self-Powered Radio Tags for Building-Scale Activity Sensing. In *Proceedings of the 32nd Annual ACM Symposium on User Interface Software and Technology*. 973–985.

[84] Kening Zhu and Shengdong Zhao. 2013. AutoGami: a low-cost rapid prototyping toolkit for automated movable paper craft. In *Proceedings of the SIGCHI conference on human factors in computing systems*. 661–670.